The Colors of the Deep Sky

Thor Olson ▲
Electronics for Imaging, Eagan, Minnesota, USA

The equipment needed to take astronomical images of deep sky objects, those faint targets found only with optical assistance, is within the reach of dedicated amateur astronomers. In such low light levels there is no color, strictly, but there is a natural desire to make these images look as they might appear if our vision were sensitive enough to perceive color. This is a component of esthetic presentation, and the use of color for this subject is extremely useful in education. CCD imaging equipment allows us to record and measure the spectral energy in a specific band determined by a filter placed in front of the sensor. By making several such recordings through red, green, blue, and sometimes additional filters, a full color composite can be created. Of particular interest are emission nebulas, whose spectra comprise the lines of energized gases. These are present in a scene along with the broadband blackbody emissions of stars. Because the spectra of these objects are simple or well known, they can be modeled and their recordings calibrated. Conventional color science methods can then be used to generate colorimetrically correct renditions of the scene.

Journal of Imaging Science and Technology, 47: 517–524 (2003)

Background and Fundamentals

It is a well known principle in color reproduction theory that to faithfully reproduce a scene containing arbitrary spectra, the detector must span the vector space of the human visual system. In practice, real world detectors are limited by the physics of filters and transducers, and true colorimetric systems are not commercially available.

In the case of astrophotography, there is an opportunity to make very close reproductions of the scene. It must be stated here however that the "true" representation of the color of these extended objects is a deception. Were we to see them with our own eyes, even at the eyepiece of a powerful telescope, we would see only pale hints of color if we see any at all. The nebulae and galaxies that we can see and record are faint extended objects in space. If we could get closer to them, they would appear larger, but no brighter, as the energy they emit is spread over an ever larger, more diffuse angular area. There is no vantage point where a human could ever directly see their color. Hence, by definition, they have no color.

Nevertheless, we can imagine the light being amplified, or our eyes being sensitized in some way that if we were to see color, what it would be. Further, we can render it using the channels recorded by a CCD detector through its filter set. What makes this possible, in spite of the general requirement for colorimetric detectors, is that the light we are recording does not contain arbitrary spectra as in a sunlit scene on our planet, it is actually very simple; it can be modeled with only a few known and constant spectral components.

To determine the requirements for detecting and rendering astrophotos with colorimetric accuracy, we will use the tools of linear vector spaces. An excellent and concise presentation of this topic and its application to color reproduction is given by Horn.[1] He proves a number of useful color reproduction theorems, starting with detector requirements. While the detector response to reproduce the appearance of arbitrary spectra needs to span the human visual functions, there is no such requirement on the primaries of the display device, a happy situation that has allowed many diverse technologies to be used on the output side of reproduction.

Many popular astronomical scenes contain objects which have well known spectra. Obviously there are stars which can be portrayed for visual purposes by spectra of black body radiators.[2] A sample starfield containing mu-Cephei, the "garnet star" is shown in **Color Plate 5(a), p. 588**. The colorful range of stars shows up nicely on some film images, a function of how the three color sensitive film layers record their continuous spectral power distributions. A sampling of these spectra are shown in Fig. 1, which shows the spectral shift between low and high temperature radiation. Mu-Cephei might be more properly called orange, but is declared by some observers as garnet by virtue of its contrast to the high temperature blue stars nearby.

Also popular are emission nebulas, large regions of excited gas that emit light at specific characteristic wavelengths. A dominant emission is the primary line of hydrogen, H-alpha at 656 nm. Also commonly found

Original manuscript received January 27, 2003

▲ IS&T Member

Color Plates 5– 12 are printed in the color plate section of this issue, pp. 586–603.

Supplemental Materials—Figures 1– 8 can be found in color on the IS&T website (www.imaging.org) for a period of no less than two years from the date of publication.

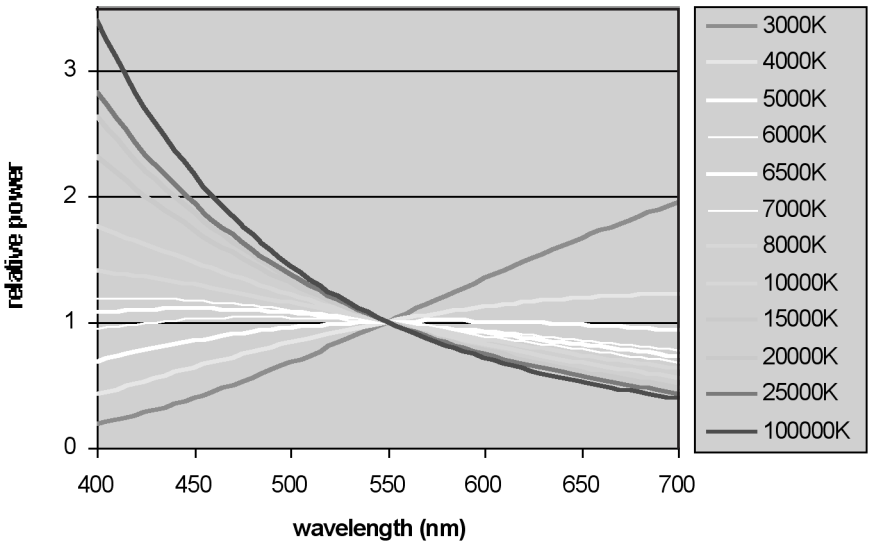

Figure 1. The spectral power distribution of most stars is dominated by the black body radiation of its surface, characterized by its temperature. Here is a sampling of these spectral shapes, normalized to have the same amplitude at 550 nm. *A full color version of this figure can be found as Supplemental Material on the IS&T website (www.imaging.org) for a period of no less than two years from the date of publication.*

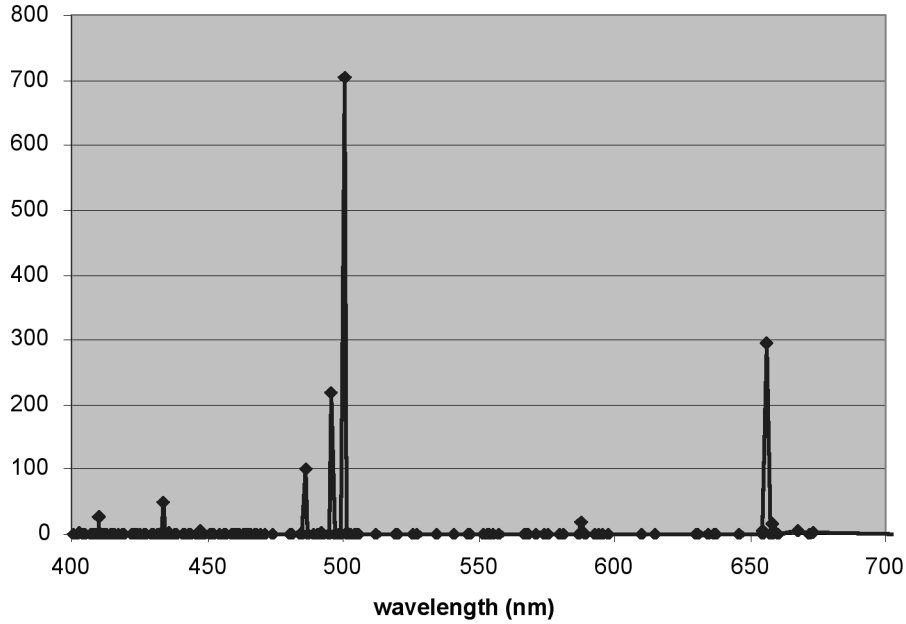

Figure 2. A spectrum for an emission nebula, specifically, NGC 6543, the Cat's Eye Nebula. The dominant lines are for H-alpha (hydrogen) at 656 nm, O-III (doubly ionized oxygen) at 501 and 496 nm, and H-beta at 486 nm. There are other contributing elements, but at lesser amplitudes. This is not identical to the spectrum for the Veil nebula, but the dominant lines are similar. *A full color version of this figure can be found as Supplemental Material on the IS&T website (www.imaging.org) for a period of no less than two years from the date of publication.*

are H-beta, at 486 nm, and ionized oxygen, O-III at 501 nm.[3,4] **Color Plate 5(b), p. 588** shows a film image of the Veil Nebula, a supernova remnant that emits energy at all three of these wavelengths. Figure 2 shows a detailed spectrum of another nebula, the Cat's Eye nebula. The same three emission lines are apparent, as well as many smaller amplitudes representing electron-transitions in other elements.

A third large category of deep sky objects are reflection nebulas, regions of interstellar space populated with dust that reflects the light from nearby stars. **Color Plate 5(c), p. 588** shows a film image of a colorful region near rho-Ophiuchus. Scattering by interstellar dust results in a "blue-shift" of the starlight (see Fig. 5).

We will discuss the colorimetric rendering of these various deep sky objects, focusing primarily on emission nebula, but the theory developed will accommodate the broadband sources of stars and reflection nebula as well.

Conventional Astrophotography

What are the traditional ways for capturing and displaying astrophotographic subjects? Probably the most widely used method for capturing these objects also has the longest history: photographic film. More recent tech-

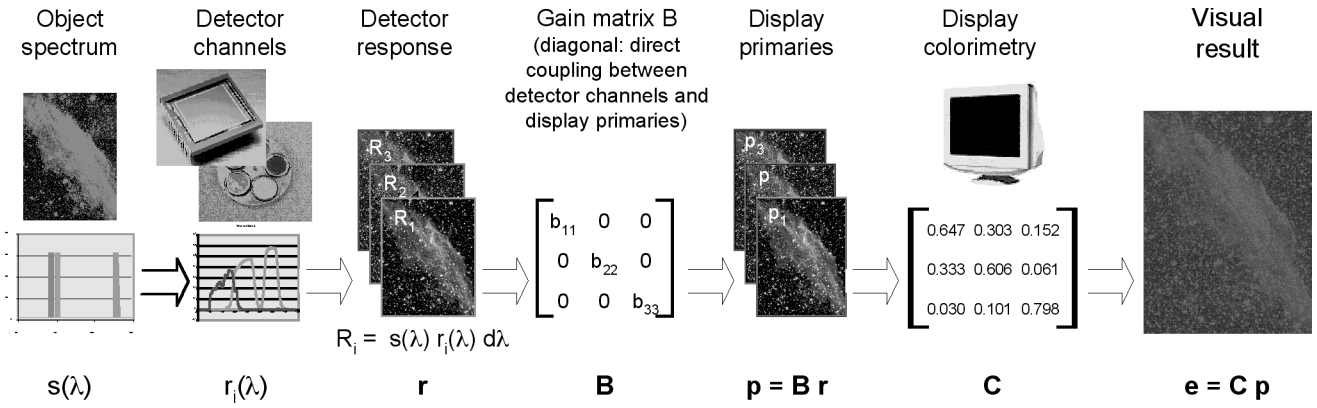

Figure 3. Schematic representation of typical asrtrophotographic imaging. Typically, the picture is "color balanced" by adjusting individual gains of the channels to make the stars look "white". The astrophotographer does not really implement a (diagonal) B-matrix to do this, rather the detector channel recordings are connected directly to the display primaries, resulting in a colorimetrically-incorrect rendition. *A full color version of this figure can be found as Supplemental Material on the IS&T website (www.imaging.org) for a period of no less than two years from the date of publication.*

niques utilize silicon CCD sensors with a linear, rather than power law response to the low level signals. Creating a color image requires either color separation filters, or the built-in spectral responses of the layers in color film.

Whether film or CCD, both use a spectrally sensitive capture device to generate distinct channels of data from the detector. In either case, contemporary practitioners of this craft will typically obtain three records of the scene corresponding to wideband RGB samples of its spectrum. These are then "color balanced" to create an RGB image suitable for display or print.

Figure 3 shows schematically the equivalent functional steps in obtaining the picture. There are a couple of items to note in this procedure. First, the spectral sensitivity of the detector channels may not be particularly suited to recording certain types of spectra. In particular, while the wideband responses in color film is quite suitable for broadband emitters like the sun and stars, its design for rendering beautiful natural scenery and pleasing fleshtones results in a spectral sensitivity having a significant gap exactly where the important O-III emission line radiates (501 nm). This is a serious problem for astrophotographers using commercially available color film trying to capture O-III emission nebulas. The workaround is to use panchromatic black and white film with suitable filters that don't miss this region of the spectrum, or to use those filters on a silicon detector that is sensitive across the full visible spectrum.

The second item to note is that the color balancing step is performed as a one-dimensional adjustment. The relative signal amplitudes in the three records are adjusted to compensate for sensitivity differences in the channels. These differences arise from many sources. In film it is dominated by reciprocity law failure that comes from lengthy exposures; the loss of response for such low level signals is different in each film layer. In silicon detectors, the non-flat response of the sensor, and the differing transmissions of the color filters must be compensated. The method typically used for finding the correct color balance is to empirically adjust the amplitude levels in each channel until the background becomes neutral, and the stars are mostly "white". The resulting image may be *called* calibrated by its author, but it obviously cannot be considered colorimetrically calibrated.

Colorimetric Requirements for a Three Channel Detector

To illustrate how to meet the requirements for colorimetric accuracy, consider an astronomic scene where there are only three components of light, say two line sources, H-alpha and OIII, and the uniformly flat spectrum, "*E*", representing a broadband source. The spectrum of the light in this scene reaching any given pixel will comprise three weighted components:

$$S(\lambda) = \sum_{i=1}^{3} F_i f_i(\lambda) \tag{1}$$

where $f_1 = 1$
$f_2 = \delta(656)$
$f_3 = \delta\,(501)$

and F_1, F_2, and F_3 are the "amounts" of each of the source illumination functions.

We take three recordings of this spectrum through three filters. Each filter, combined with the detector spectral sensitivity, has a response of $r_j(\lambda)$. Each of these channels sees the light source spectra differently, their output will be:

$$r_i = \sum_{j=1}^{3} F_j \int f_j(\lambda) \cdot r_i(\lambda) d\lambda \tag{2}$$

In vector notation:

$$\mathbf{r} = \mathbf{H}\,\mathbf{f} \tag{3}$$

where **r** and **f** are column vectors and the elements of matrix **H** are:

$$h_{ij} = \int r_i(\lambda) f_j(\lambda) d\lambda \tag{4}$$

A human eye sees the spectrum through three channels as well, their responses are the color matching functions $e_i(\lambda)$. The three outputs of this system are tristimulus values:

$$e_i = \sum_{j=1}^{3} F_j \int f_j(\lambda) \cdot e_i(\lambda) d\lambda \tag{5}$$

The vector version is:

$$\mathbf{e} = \mathbf{G}\,\mathbf{f} \tag{6}$$

With the elements of **G**:

$$g_{ij} = \int e_i(\lambda) f_j(\lambda) d\lambda \tag{7}$$

Solving Eqs. (3) and (6):

$$\mathbf{e} = \mathbf{G}\,\mathbf{H}^{-1}\,\mathbf{r} \tag{8}$$

So we can compute the tristimulus **e** of this (spectrally limited) scene which produced detector output **r**.

When we want to present the scene on a display that uses three primary (typically RGB) light sources, characterized by the vector equation:

$$\mathbf{e} = \mathbf{C}\,\mathbf{p} \tag{9}$$

we solve for the drive levels of the primaries, **p**, for the desired tristimulus:

$$\mathbf{p} = \mathbf{C}^{-1}\,\mathbf{e} \tag{10}$$

And if we set the output tristimulus vector to the tristimulus of the original scene, we obtain our desired result:

$$\mathbf{p} = \mathbf{C}^{-1}\,\mathbf{G}\,\mathbf{H}^{-1}\,\mathbf{r} \tag{11}$$

The matrices can be combined into a single operator, **B**, that relates the detector channels to the display channels:

$$\mathbf{p} = \mathbf{B}\,\mathbf{r}; \qquad \mathbf{B} = \mathbf{C}^{-1}\,\mathbf{G}\,\mathbf{H}^{-1} \tag{12}$$

The reproduction of pure tristimulus values in the system above does not account for white point adaptation between the original scene and its presentation on the display system described by **C**. Implicit in this model is that the (virtual) observer of the astronomic scene is adapted to the display whitepoint (D65 for sRGB), a questionable assumption for any observation at scotopic levels, but consistent with the nature and spirit of this academic exercise in colorimetry.

So we now have a simple means to obtain an image for a specific display (or RGB color space), directly from the recorded channels of a given multiband image sensor. It will be colorimetrically correct to the degree that the scene can be represented by the basis functions assumed in $f_j(\lambda)$.

Scenes with More than Three Spectral Components

What if the scene is more complex than the simple three-component set of light sources we assumed above? Say we wanted to include a third or fourth emission line, or, as will be described later, the broadband sources are represented by a superposition of three bases instead of the simple "*E*" flat spectrum. The additional components are included in a larger model for the source spectrum:

$$S(\lambda) = \sum_{i=1}^{N} F_i f_i(\lambda) \tag{13}$$

To resolve the higher *N*-dimensional spectrum, we need *N* independent detector channels, each with its particular spectral sensitivity, $r_j(\lambda)$. The detectors need not single out each component of the illuminant spectrum, but collectively they must span its vector space. This is so that the relation between them (Eqs. (2)–(4)) can be inverted, that is, $\mathbf{H}^{-1}$ must exist.

The transform matrix **G** that obtains the tristimulus vector is evaluated as before by Eq. (7), but now there are N cross products with each color matching function, and the matrix becomes $3 \times N$. It is always used in this form, no inverse, or pseudo-inverse is needed. The solution for the overall transform **B**, between detector channels and display channels yields a similar $3 \times N$ matrix.

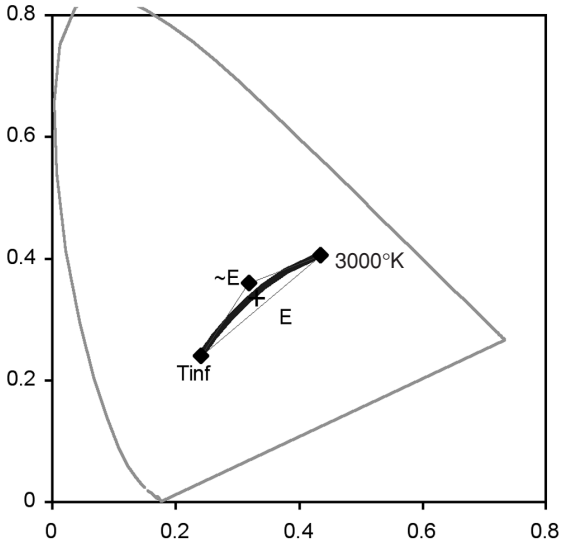

Figure 4. The locus of blackbody colors from 3000°K to T_{inf} on the chromaticity diagram. Point ~*E* is the location of a complementary power distribution which, when combined with 3000°K and T_{inf}, results in a "whitepoint" of *E*, the flat equi-power spectrum (+ symbol). The resulting gamut of this three primary system is an efficient container for the blackbody locus. *A full color version of this figure can be found as Supplemental Material on the IS&T website (www.imaging.org) for a period of no less than two years from the date of publication.*

Some Suitable Illumination Source Models

Stars, even though their detailed spectra are quite complex, are well represented by a blackbody emission spectra. And reflection nebula, are really just regions of space that reflect the light from nearby stars. Can these objects be approximated by a superposition of linear basis spectra?

Figure 4 shows the chromaticity locus of blackbody spectral power distributions. Over the region 3000°K to T_{inf}, the chromaticity follows a gentle path. If we take these endpoints and find a suitable third spectral "primary" to mix in, we could approximate the spectral shapes found along this path. Figure 5 shows a candidate: the spectral waveform, ~*E*, that when added to those of 3000°K and T_{inf} yields "*E*", the flat spectral distribution. This set of basis waveforms will be referred to as the "3Ei" set indicating their linearly independent components (3000°K, ~*E*, T_{inf}). *E* is actually the "whitepoint" for this three-component system. Figure 4 shows the chromaticity "gamut" of 3*Ei*, which contains the blackbody locus very efficiently. The 3*Ei* basis set can represent all of the stars in an astrophoto.(at least those that have an effective blackbody temperature between 3000°K and infinity).

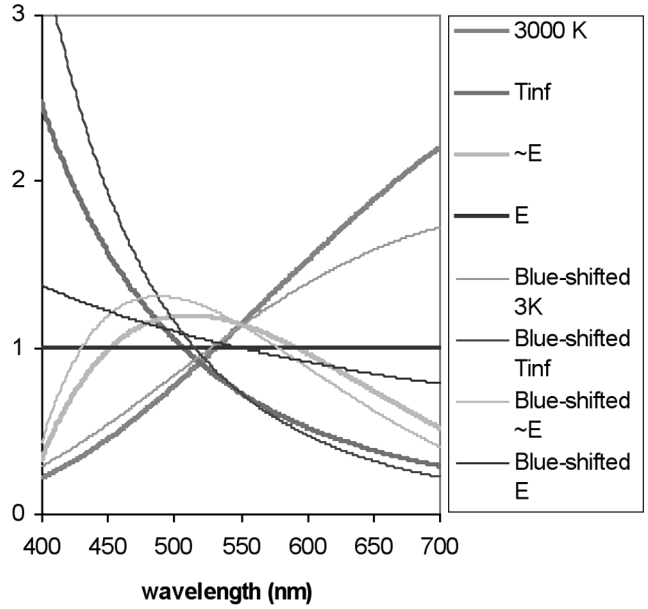

Figure 5. The "3*Ei*" basis spectra (bold curves). They sum in equal parts to form the flat *E* spectrum, and blackbody spectral shapes are approximated by suitable sums of them. Also shown, the effect of Mie scattering: the 3*Ei* basis waveforms are blue-shifted (thin lines) by the $1/\lambda$ scattering of reflection nebula material. *A full color version of this figure can be found as Supplemental Material on the IS&T website (www.imaging.org) for a period of no less than two years from the date of publication.*

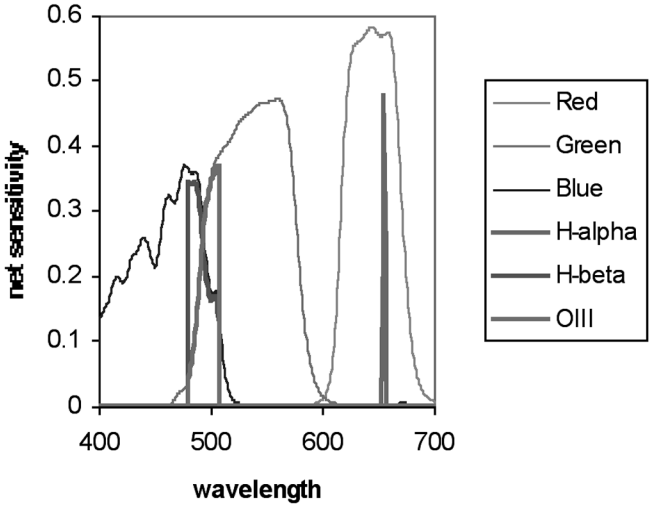

Figure 6. Net detector charactreristics used to obtain Mike Cook's image frames of the Veil Nebula. This is the composite of filter transmission, silicon sensitivity, and atmospheric extinction. *A full color version of this figure can be found as Supplemental Material on the IS&T website (www.imaging.org) for a period of no less than two years from the date of publication.*

When stars are in a region of relatively dense dust and gas in the interstellar medium, their light is scattered, giving rise to deep sky objects called *reflection nebula* (as opposed to emission nebula whose energized gas is actively emitting light). Astronomers have learned that these regions are dominated by Mie scattering: the light is preferentially reflected according to a $1/\lambda$ law. The light source could be a star of any temperature, and reflection nebulae are collectively wide ranging and colorful deep sky objects.

Because they are illuminated by their nearby stars, reflection nebula spectra should be a composite of them, modified by their $1/\lambda$ characteristic. Applying the scattering function to the 3*Ei* basis spectra, we obtain the second set of spectra in Fig. 5, blue-shifted versions of the blackbody spectra. Their visual response and location on the chromaticity diagram is shifted only slightly from the blackbody colors, but it is important to maintain this distinction, the detector channels will see these spectra rather differently than people.

We now have an assortment of basis functions to use for the illumination model of the scene. The 3Ei set is appropriate for stars, their blue-shifted versions for reflection nebula, and delta functions at the appropriate wavelengths for emission nebulas. Not all are needed in every scene, and new ones may be required for more exotic situations. Because the scenes have known spectra, we can represent them with these linear models, and obtain a simple method to display their image in a colorimetrically correct manner. An example of this is given in the next section.

A First Application

To test this attractively simple result and illustrate its application, a set of astronomical image frames was obtained as source data. The image is of the Veil Nebula, a supernova remnant comprising a shell of ionized gasses that emit in H-alpha, H-beta and O-III spectral lines. The images are by astrophotographer Mike Cook who used an SBIG ST10 CCD detector equipped with three wideband red, green and blue filters, and three narrowband filters that isolate and pass the emission lines.

There are additional factors that influence the sensitivity functions $r_j(\lambda)$ of the detector. These include the spectral sensitivity of the silicon photodetector array, and the "atmospheric extinction", that characteristic of the air that makes the sun look yellow in a sky of blue, reddening as it approaches sunset.[5] The net detector response of the six channels is shown in Fig. 6.

The 3*Ei* spectral basis set (described prior) was used to represent the stellar light sources. Another model of illumination for the line-spectra emissions was made from a simple set of delta functions at the wavelengths 656, 501, and 486. Keeping with three-letter acronyms, these bases form the "a3b" (H-alpha, O-3, H-beta) set.

Looking first at the wideband red, green, and blue rgb (lower case rgb) filtered images, we can form the various cross-product integrals of the detector response with the light source. If we use the 3*Ei* broadband light source model we get a 3*Ei*-to-rgb version of **H**. Similarly, we can form **G**, the cross-products of the 3*Ei* broadband light source bases with the color matching functions. Selecting AdobeRGB for the RGB display space (uppercase RGB) for **C** gives us everything we need to evaluate Eq. (12). The resulting matrix is:

$$\mathbf{B}_{rgb-3Ei-RGB} = \mathbf{C}^{-1}\mathbf{G}\mathbf{H}^{-1} = \begin{bmatrix} 2.470 & 1.237 & -0.352 \\ -0.093 & 2.985 & -0.514 \\ -0.100 & -0.376 & 4.120 \end{bmatrix} \quad (14)$$

This matrix is essentially just a transform from the color filter channels, rgb, to the display space prima-

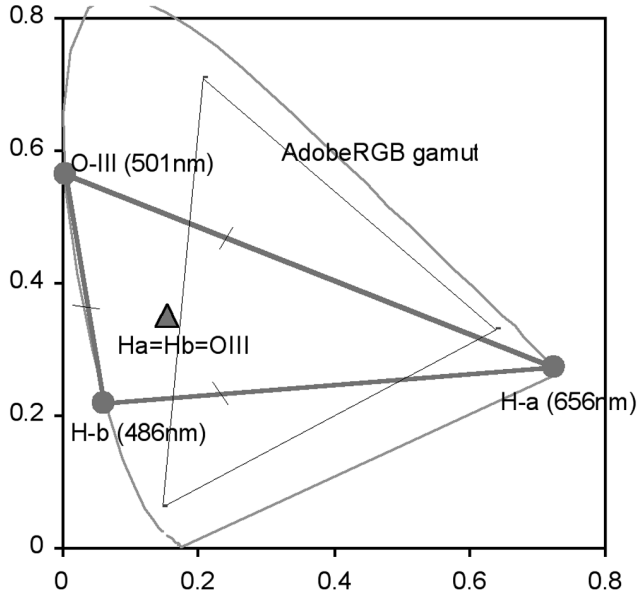

Figure 7. The gamut of colors possible from the "a3b" emission lines sources. The "whitepoint" of the a3b system, where equal-energy amounts of each emission line contribute, marked by the triangle, falls just outside the blue-green boundary of the AdobeRGB gamut. *A full color version of this figure can be found as Supplemental Material on the IS&T website (www.imaging.org) for a period of no less than two years from the date of publication.*

ries RGB. An RGB scanner would (should) use a similar system.

If we go through the same procedure but using the a3b emission-line light source model, we get the matrix:

$$\mathbf{B}_{rgb-a3b-RGB} = \begin{bmatrix} 0.665 & -0.583 & -0.353 \\ -0.101 & 1.614 & 0.330 \\ -0.012 & -0.161 & 1.649 \end{bmatrix} \quad (15)$$

These weighting matrices can now be applied to the rgb image frames. In practice, CCD images are obtained with varying exposures times. To maintain calibration, the data must first be divided by the relative exposure so that the image channels are on a common scale. Other practical issues that must be addressed include establishing the zero level of the data, and removing any residual scale factors. Fortunately CCD sensors are linear detectors, easing the effort to bring the data into a calibrated linear signal space.

Color Plates 6(a) and 6(b), p. 588 show the application of these color conversion matrices to a portion of the Veil image. After performing the operation, the resulting image data was scaled to where the low-level emission signal becomes visible, though the high intensity stars saturate. The first image shows a picture typical of many photographs of the Veil Nebula, a delicate red cloud hanging among the stars. The stars are correctly rendered, but the nebula itself is not.

Color Plate 6(b), p. 588 shows an image from the same source data, but the line emission transform was applied. In this case the nebula is correctly rendered, but the stars are all blue-green! This is actually their correct representation in this system: a broadband source like a star would contribute roughly equal amounts of energy at the three emission line wavelengths. The chromaticity location of equal spectral amplitude levels of the a3b primaries is shown in Fig. 7, just outside the blue-green edge of the AdobeRGB gamut.

While the above example shows that one can obtain the correct nebula colors from a wideband rgb image, it is beneficial from the standpoint of signal to noise ratios, to render the nebula from a set of narrowband detector images. The same analysis applies, this time the cross-products are with the narrowband filter responses (call the filtered channels Ha, O3, Hb). For Mike Cook's system, the matrix result is:

$$\mathbf{B}_{HaO3Hb-a3b-RGB} = \begin{bmatrix} 0.800 & -0.614 & -0.372 \\ -0.118 & 1.699 & 0.347 \\ -0.013 & -0.169 & 1.736 \end{bmatrix} \quad (16)$$

The image (**Color Plate 6(c), p. 588**) has the same characteristically blue-green stars, but the details and amplitude in the nebula itself are more pronounced, and the strong colors of the emission lines stand out.

A Less Simple Application

How can one obtain both correct nebula colors and correct star colors? By using all six recordings of the scene (both sets of narrowband and wideband filtered channels), we can calculate the matrix that combines them and use it to generate a calibrated RGB result. When all of the sensitivities and cross-products are evaluated, the B matrix is now:

$$\mathbf{B}_{rgbHaO3Hb-3Eia3b-RGB} = \begin{bmatrix} 2.486 & 1.660 & -0.186 & -2.198 & -2.355 & -0.167 \\ -0.122 & 3.113 & -0.492 & 0.024 & -1.578 & 0.865 \\ -0.259 & 0.134 & 4.363 & 0.293 & -0.311 & -2.858 \end{bmatrix} \quad (17)$$

The RGB display image is obtained by operating on the column vector formed by the intensities from the six channels (wideband r, g, b, narrowband Ha, O3, Hb) with the 3×6 B matrix.

$$\begin{bmatrix} R \\ G \\ B \end{bmatrix} = \begin{bmatrix} b_{11} & b_{12} & b_{13} & b_{14} & b_{15} & b_{16} \\ b_{21} & b_{22} & b_{23} & b_{24} & b_{25} & b_{26} \\ b_{31} & b_{32} & b_{33} & b_{34} & b_{35} & b_{36} \end{bmatrix} \bullet \begin{bmatrix} r \\ g \\ b \\ Ha \\ O3 \\ Hb \end{bmatrix} \quad (18)$$

The result is quite disappointing (**Color Plate 7(a), p. 589**). The high amplitude stars are ok, but the nebula does not reveal the colors we have come to expect from **Color Plates 6(b) and 6(c), p. 588**, instead, returning to the dominating red cloud that obscures the blue-green components from O-III and H-beta. Why should this be so?

A clue is found by examining the components of the B matrix and how they operate on an input 6-vector (Eqs. (17) and (18)). It can be seen that the contributions from the narrowband channels are largely *subtracted from* the signal amplitudes obtained from the wideband

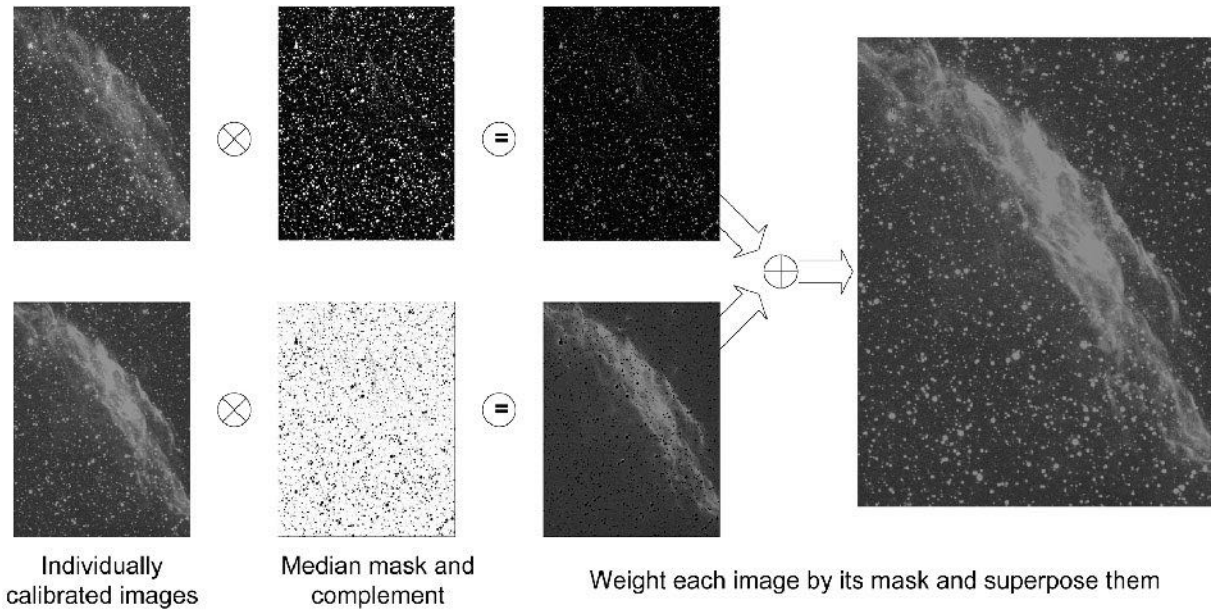

Figure 8. A spatial method to combine two images calibrated separately to different source illumination assumptions. The wideband rgb records of blackbody radiation model 3Ei, top, and the narrowband HaO3Hb records of emission line model a3b, bottom, are multiplied by a mask and its complement, then summed. The mask was obtained by a medium filter operating on the rgb source data. *A full color version of this figure can be found as Supplemental Material on the IS&T website (www.imaging.org) for a period of no less than two years from the date of publication.*

records. This suggests that the information obtained from the wideband channels *overestimates* the emission line illumination amplitudes, which is then corrected by subtracting their (more accurately obtained) measurements by the narrowband channels.

A second clue was found by examining the raw recordings of the wideband red and the narrowband H-alpha data. Regions of the image that were identified as containing only H-alpha emission energy were recorded as having a much higher intensity in the wideband than in the narrowband channel, about twice as much! If H-alpha emission is truly a delta-function, as we are modeling it, the two recordings of this emission line should be about the same between the two channels. Where is the extra light in the wideband recording coming from, or conversely, why is the narrowband channel not recording it all?

The Veil nebula is expanding with a remarkably fast velocity, some regions in excess of 100 km/s, resulting in spectral broadening of its emission lines.[6] In this case the lines are so broadened, that much of the energy now falls outside the 3 nm bandwidth of Mike Cook's H-alpha filter. So here we have an example (**Color Plate 7(a), p. 589**) of what results from our calibration method when the actual illumination in a scene is not properly represented by our model of it.

To get an estimate of what we might see with an improved illumination model, the delta function for representing the H-alpha emission line was replaced by a gaussian-broadened line that spilled half of its energy outside of our 3 nm filter bandwidth. This change impacts the coefficients in the B matrix only slightly (compare Eq. (19) with Eq. (17)), except for a large change in the contribution to R from the narrowband Ha channel (b_{14}). The data from this channel are now more strongly subtracted, reflecting the fact that the H-alpha record is undersampling the total H-alpha energy:

$$\mathbf{B}_{rgbHaO3Hb-3Eia3b-RGB} = \begin{bmatrix} 2.651 & 1.658 & -0.163 & -5.131 & -2.343 & -0.177 \\ -0.124 & 3.113 & -0.492 & 0.054 & -1.578 & 0.865 \\ -0.281 & 0.134 & 4.360 & 0.685 & -0.312 & -2.857 \end{bmatrix} \quad (19)$$

The RGB image computed using this version of the B matrix (**Color Plate 7(b), p. 589**) shows that the nebula is nearly gone! If we amplify the image further (**Color Plate 7(c), p. 589**) we find that while the nebula's color is now similar to what we have come to expect, its overall amplitude has been lost in the noise. This seems to be a difficulty when combining image channels that have different signal to noise ratios. The problem is that the signal from the faint emission line nebula is drowned in the noise from a wideband spectral sensor. This was suggested by the relative appearance of **Color Plates 6(b) and 6(c), p. 588**, which portray the emission sources using data from only the wideband, large-noise channels, and then from the narrowband, low-noise detectors. The narrowband set permits an overall larger gain to be used, because of its larger signal to noise ratio. In effect, we are able to see "deeper" into this deep sky object with the narrowband detectors, albeit requiring a longer exposure time.

Combining Results

Must we accept excessive noise in the pursuit of our goal to achieve color accuracy? The difficulties in matching signal and noise characteristics between channels is a problem yet to be solved, but in the meantime, a spatial filtering method has been successfully used to combine the best results from the calibration efforts above.

If the broadband sources (the stars) in the image could be identified, one could select the appropriate image, e.g., **Color Plates 6(a) or 6(c), p. 588**, from which to

select rendered pixels and merge them in a composite result. It is tempting to use a color selective method to generate a spatial mask, by identifying all those out of gamut blue-green pixels, for example, that result from stars being interpreted as a3b sources. This was found to be not reliable, since there are legitimate a3b sources in the nebula region that look the same.

Instead, a spatial filtering method was used, schematically depicted in Fig. 8, in which a median filter was used to remove small point-like sources. The complement of this filtered image identifies the stars. By appropriate scaling, this becomes a useful mask, permitting a mixing between the two source images and obtaining a picture that has a colorimetrically rendered nebula among correctly tinted stars (**Color Plate 8, p. 589**).

The image is an unusual portrayal of this famous deep sky object. The energy associated with the leading shock front is vividly shown by the blue-green emissions of ionized oxygen, with the red, lower energy hydrogen trailing behind it. Most images easily capture the red but under-represent this color of green. Color film is nearly blind to this spectral line, and silicon has great sensitivity to deep red, but even when recorded at correct amplitude, the Veil will be misrendered by a naive calibration that tries to make stars look natural.

A Gallery of Colorimetrically-Rendered Images

We can apply the principles of colorimetric rendering to other astrophotos, but as we have seen, it is very important to maintain careful exposure and spectral calibration of the detector that is making the recordings. Mike Cook is a fastidious and skilled amateur astronomer, making it possible to apply the methods to his data. Another source of well calibrated data is the Hubble Telescope, whose archives are public and available to those willing to navigate the arcane procedures to turn them into useful image files. A set of images was obtained and processed using the (3-channel) techniques described in this article (**Color Plates 9 through 12, p. 590**). The images are quite famous, and their press release version and public relations information are shown for comparison. The captions provide annotation.

Conclusions

Many popular astrophotographics subjects comprise simple or well known spectra as their subject matter. Because of this, it is possible to generate colorimetrically correct renditions of them (unlike natural scenery on our planet). By modeling the illumination sources, and knowing the spectral response of our detector, we can generate calibrated RGB images.

The spectra of blackbody radiators, i.e., stars, can be approximated using a three-component set of spectral basis functions: essentially the spectrum from a 3000K radiator, one at infinite temperature, and the uniformly flat E-spectrum. Emission line spectra are modeled by delta functions, though for some objects, this may be too simple. As we saw with the Veil Nebula, the actual line source was broad enough to fall partially outside our detector band, an argument perhaps to use a slightly wider filter to capture the energy from line sources.

It is possible to obtain colorimetric renderings of broadband and of line emitting sources, but in attempting to do both in a single matrix operation we found that low level signals became lost in the noise of the wideband detector channels. An alternate two-step procedure using spatial superposition can get around this problem for some scenes where the two source types can be adequately segmented.

While the application of colorimetric rendering methods to astrophotographs does not advance the science of astronomy, it can enhance our ability to present and explain it. The educational aspects and the esthetic component of visual accuracy are benefits to be gained. The principles for exact reproduction are well known but usually not of widespread or of practical interest because of the spectral complexity in most subjects. Here is a subject that is spectrally simple (except perhaps to a professional astronomer) and can actually be exactly rendered. ◬

Acknowledgment. I am indebted to Mike Cook for contributing his full resolution image frames to this project and guiding me through an explanation of their exposure. Some of Mike's other technically challenging activities are presented on his website: http://www.af9y.com. Jerry Lodriguss (http://www.astopix.com) provided the film images to illustrate some other splendors of the universe.

Color Plates 9 through 12, p. 590 were based on observations made with the NASA/ESA Hubble Space Telescope, obtained from the data archive at the Space Telescope Science Institute. STScI is operated by the Association of Universities for Research in Astronomy, Inc. under NASA contract NAS 5-26555.

Thanks also to the anonymous reviewers for their suggestions to improve the clarity of this presentation.

References

1. B. K. P. Horn, Exact Reproduction of Colored Images, *Computer Vision, Graphics, and Image Processing* **26,** 135–167 (1984).
2. T. Olson, The Colors of the Stars, *Proc. IS&T/SID Sixth Color Imaging Conference*, IS&T, Springfield, VA, 1998, pp. 233–240.
3. D. Malin and P. Murdin, *Colours of the Stars*, Cambridge University Press, Cambridge, UK, 1984.
4. D. Malin, *A View of the Universe*, Sky Publishing Corp and Cambridge University Press, Cambridge, UK, 1993.
5. D. L. King, Atmospheric Extinction at the Roque de los Muchachos Observatory, La Palma, RGO/La Palma technical note no 31, 1985, http://www.ing.iac.es/Astronomy/observing/manuals/ps/tech_notes/tn031.pdf
6. W. Blair, Distance to the Cygnus Loop from Hubble Space Telescope Imaging of the Primary Shock Front, *Astronomical J.* **118,** 942 (1999).

(a) **(b)** **(c)**

Color Plate 6(a). A starfield near the Milky Way. A variety of stars of different temperatures and colors appear in this film image. Prominent near the center is a red supergiant, mu-Cephei. It is not really red, (the nearby emission nebula shows as a more true-red blob), but in contrast to its blue star neighbors in a telescopic view, mu-Cephei was dubbed the "garnet star" by English astronomer William Herschel. (Photo by the author). **(b)** A supernova remnant known as the Veil Nebula (NGC 6960/ 6992/6995). This is a film image of this emission nebula, where energized gases emit light at specific characteristic wavelengths. The example in the text utilizes a small section (small rectangle) of filtered silicon CCD exposures that originally covered the larger rectangular region indicated. (Photo courtesy Jerry Lodriguss). **(c)** The rho-Ophiuchus region where dust reflects the light from nearby stars. The areas are known as reflection nebulae, and their color is determined by the temperature of the stars shining onto them, and the scattering characteristics of the dust. (Photo courtesy Jerry Lodriguss) (*Olson*, pp. 522 – 529)

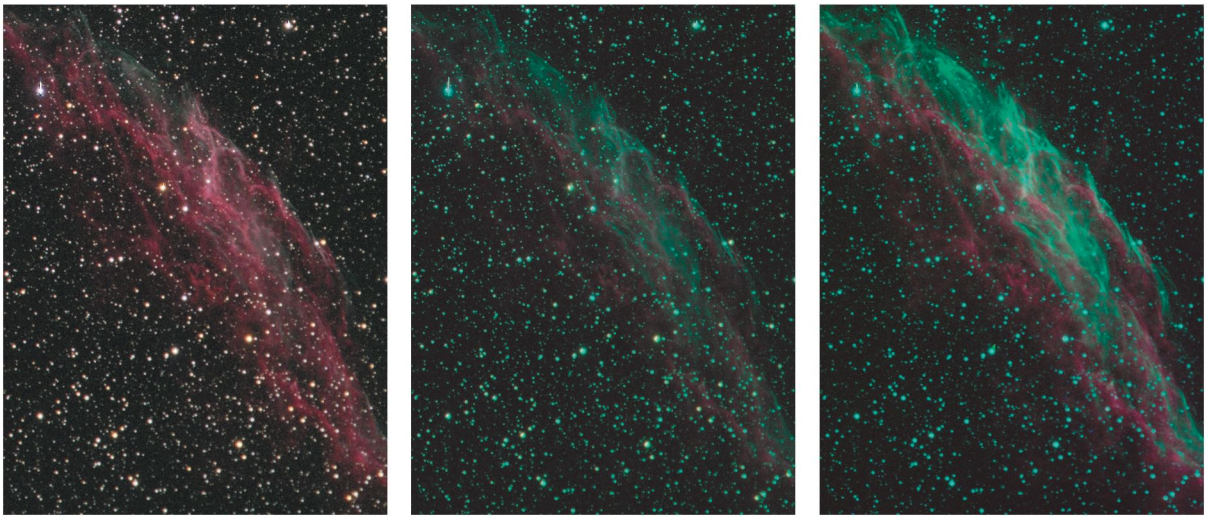

(a) **(b)** **(c)**

Color Plate 7(a). A portion of the Veil nebula rendered according to the first of two different light source assumptions. This image used the wideband rgb recordings and assumed the broadband blackbody 3Ei model. **(b)**. A rendering using the a3b emission line set as the source illumination. The original image data is the same as Color Plate 7(a): the three wideband rgb filters. **(c)**. The same emission line source assumption as in Color Plate 7(b), but the data in this case was obtained by three narrowband detector channels, improving the signal quality. (*Olson*, pp. 522 – 529)

(a) **(b)** **(c)**

Color Plate 8(a). All six recorded image channels (three wideband and three narrowband) combined using the six-component "3Eia3b" light source model. The dominant red color was an unexpected result. **(b)**. The same recorded channel data as Color Plate 8(a), but the H-alpha emission source model was changed from a delta function to a gaussian with half of its energy falling outside of the narrowband Ha detector (see text for explanation). **(c)**. An amplitude- scaled (relative gamma of 2) version of Color Plate 8(b). The colors are closer to that expected, but the nebula's low amplitude places it in the noise of the wideband detectors. (*Olson*, pp. 522 – 529)

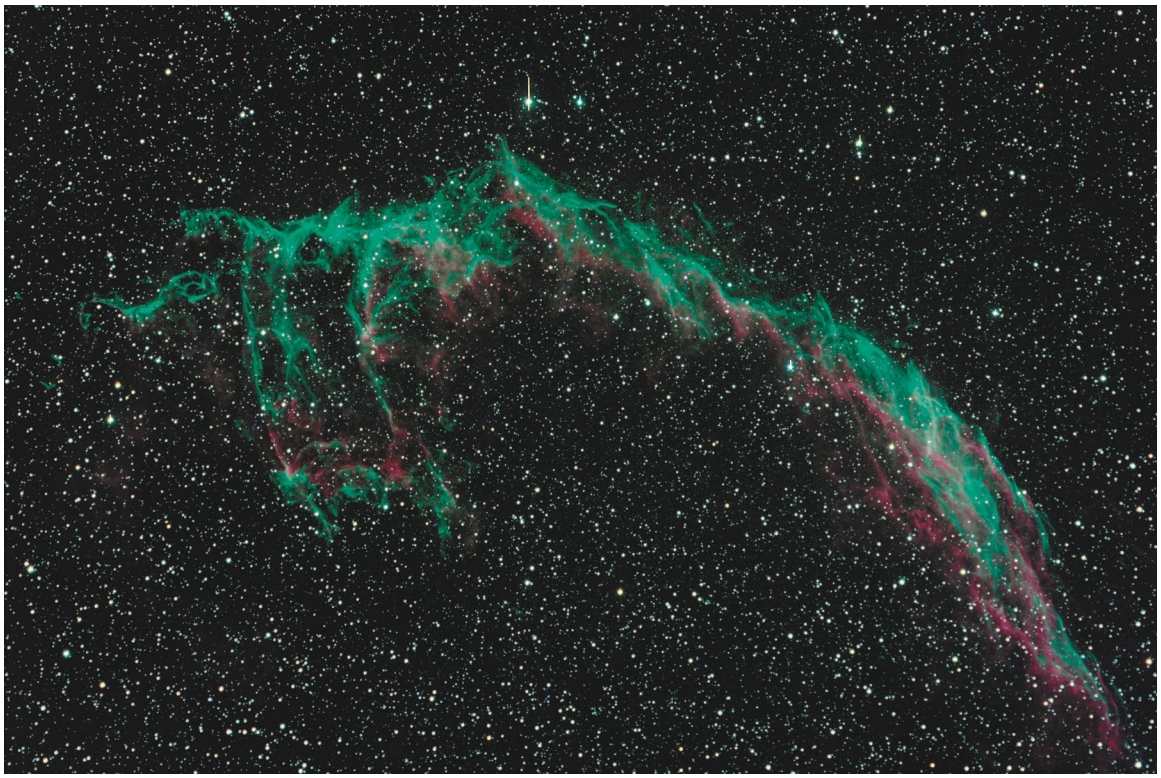

Color Plate 9. A correctly rendered Veil Nebula in a field of blackbody sources. Mike Cook used an SBIG ST-10 sensor on an Astrophysics 130mm f/6 refractor from his suburban driveway (Huntertown IN). His filter wheel is equipped with the CFW8 red, green, blue wideband filter set, and he also installed three narrowband filters to record spectral emission lines H-alpha (656 nm), ionized oxygen O-III (501 nm) and H-beta (486 nm). The image calibrated using methods described in this article. (*Olson*, pp. 522 – 529)

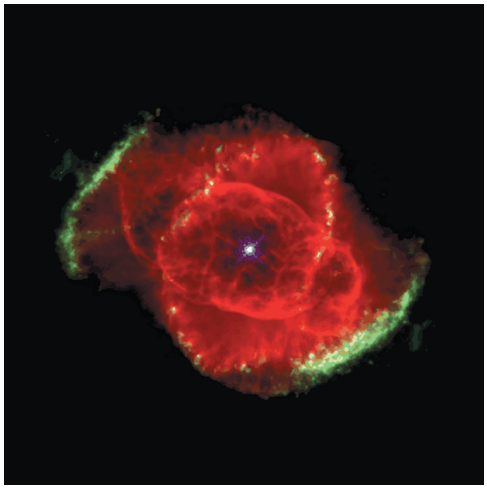

Color Plate 10. From NASA/STSci press release: "This color picture, taken with the Wide Field Planetary Camera-2, is a composite of three images taken at different wavelengths. (red, hydrogen-alpha; blue, neutral oxygen, 6300 Å; green, ionized nitrogen, 6584 Å)." NGC 6543 is also known as the Cat's Eye Nebula. All three of these wavelengths are strongly red, but when assigned to different color channels, creates a pseudocolor image that helps astronomers visualize the chemistry and physical processes going on. (*Olson,* pp. 522 – 529)

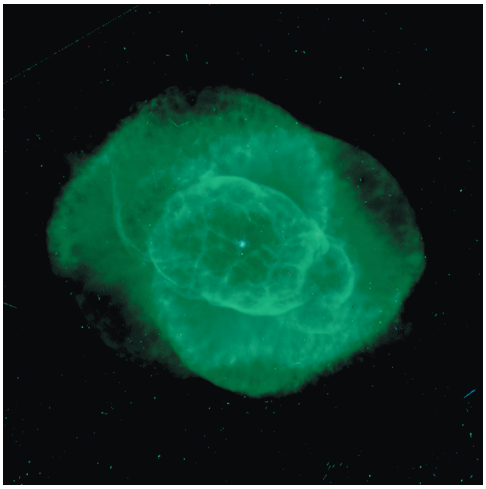

Color Plate 11. The strongest emission lines in the Cat's Eye Nebula are H-alpha, O-III, and H-beta (see Fig. 2). Hubble Space Telescope image frames from the Wide-Field Planetary Camera-2 corresponding to these lines were colorimetrically combined to obtain this "true color" view of the nebula. Although there is is significant red H-alpha energy, it is not enough to bring the combination with blue-green O-III into the RGB display gamut, and so the result is a nearly monochromatic structure in the characteristic blue-green of O-III. The bright dots and streaks in the image are artifacts from cosmic ray hits during the exposure.(*Olson,* pp. 522 – 529)

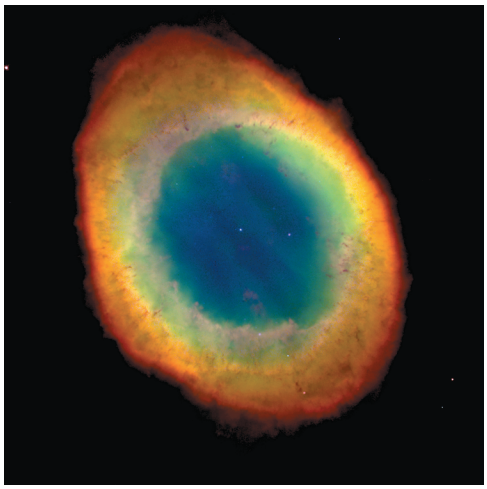

Color Plate 12. From NASA/STSci press release: "The NASA Hubble Space Telescope has captured the sharpest view yet of the most famous of all planetary nebulae: the Ring Nebula (M57). In this October 1998 image, the telescope has looked down a barrel of gas cast off by a dying star thousands of years ago. This photo reveals elongated dark clumps of material embedded in the gas at the edge of the nebula; the dying central star floating in a blue haze of hot gas. The nebula is about a light-year in diameter and is located some 2,000 light-years from Earth in the direction of the constellation Lyra." "The color image was assembled from three black-and-white photos taken through different color filters with the Hubble telescope's Wide Field Planetary Camera 2. Blue isolates emission from very hot helium, which is located primarily close to the hot central star. Green represents ionized oxygen, which is located farther from the star. Red shows ionized nitrogen, which is radiated from the coolest gas, located farthest from the star. The gradations of color illustrate how the gas glows because it is bathed in ultraviolet radiation from the remnant central star, whose surface temperature is a white-hot 216,000° F (120,000° C)." (*Olson,* pp. 522 – 529)

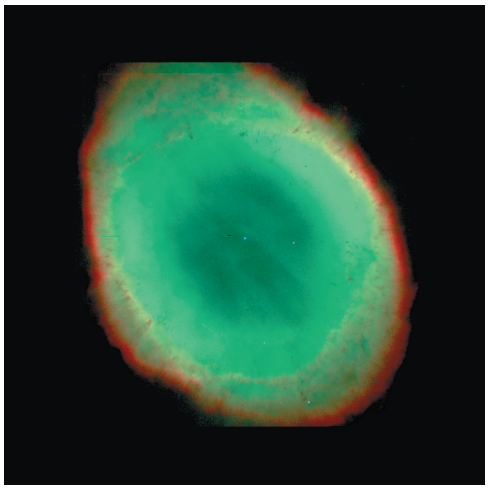

Color Plate 13. A colorimetric rendering of the same N-II (658 nm), H-a (656 nm), O-III (501 nm), and He-II (469 nm) emission lines in the Ring Nebula. The blue helium line is so weak that it contributes virtually nothing to the image, leaving the blue-green O-III to dominate until the very edge of this nebula. Not as pretty perhaps as the NASA promotional picture, but color-correct.(*Olson,* pp. 522 – 529)